Polyspecific Cation Transporters Mediate Luminal Release of Acetylcholine from Bronchial Epithelium

Katrin Susanne Lips*, Christopher Volk*, Bernhard Matthias Schmitt, Uwe Pfeil, Petra Arndt, Dagmar Miska, Leander Ermert, Wolfgang Kummer, and Hermann Koepsell

Institute of Anatomy and Cell Biology, and Institute of Pathology, Justus-Liebig-University, Giessen; Institute of Anatomy and Cell Biology, Julius-Maximilians-University, Würzburg; and Aventis Pharma Deutschland GmbH, Frankfurt, Germany

In airway epithelia, non-neuronal cholinergic regulations have been described; however, the route for acetylcholine (ACh) release has not been verified. To investigate whether organic cation transporters (OCTs) serve this function, we studied the expression of OCTs in airway epithelia and their capability to translocate ACh. Using immunohistochemistry in rats and humans, OCT1, OCT2, and OCT3 were localized to the luminal membrane of ciliated epithelial cells. In humans, OCT2 showed the strongest expression in the luminal membrane. We expressed the OCT isoforms in oocytes of *Xenopus laevis* and measured uptake and efflux of ACh. Tracer flux measurements showed that ACh is transported by OCT1 and OCT2 but not by OCT3. Two-electrode-voltage-clamp measurements revealed that OCT2 mediates electrogenic uptake and efflux of ACh. For ACh uptake by human OCT2, a K_M value of $\sim$ 0.15 mM was determined. At −50 mV, ACh efflux by human OCT2 was *trans*-inhibited by micromolar concentrations of the inhalational glucocorticoid budesonide, which is used in treatment of asthma ($K_i \sim 2.7$ μM). The data show that OCT1 and OCT2 mediate luminal ACh release in human airways and suggest that ACh release is blocked after inhalation of budesonide.

Keywords: organ cation transporters; acetylcholine efflux; bronchial epithelium; budesonide

Acetylcholine (ACh) is mainly recognized as neurotransmitter of central and peripheral neurons. Phylogenetically, however, ACh signaling evolved long before the nervous system and is involved in the regulation of basic cell functions. Besides neurons, ACh and the ACh-synthesizing enzyme choline acetyltransferase (ChAT) are found in a variety of non-neuronal mammalian cells such as epithelial cells, endothelial cells, and leukocytes (1, 2). In epithelia of the alimentary tract, airway, and skin, ACh acts as an auto- or paracrine regulator of proliferation, differentiation, and maintenance of cell–cell contacts (2). In the respiratory epithelium, ACh also increases ciliary beat frequency (3). In addition, ACh has also been identified as an autocrine growth factor for small lung cell carcinoma (4).

In contrast to the advanced understanding of ACh storage in synaptic vesicles and its release from nerve terminals, it is not understood how ACh is released from various non-neuronal cells. In both nerve terminals and non-neuronal cells, ACh is synthesized by ChAT from acetyl-CoA and choline. Acetyl-CoA is supplied by metabolism, and choline is taken up from extracellular space by the high-affinity choline transporter CHT1 (5, 6). In nerve terminals, ACh is translocated into synaptic vesicles by the vesicular acetylcholine transporter (VAChT) to await exocytotic release, which is triggered by depolarization and subsequent calcium influx via voltage-gated calcium channels. In contrast, the release of ACh from non-neuronal cells is poorly understood. Some non-neuronal cells such as human mononuclear leukocytes and leukemic T cell lines that synthesize ACh and express ChAT, do not express VAChT (7, 8). Moreover, functional evidence for vesicular storage and exocytotic release of ACh from non-neuronal cells is missing (9). Therefore, alternative mechanisms for the cellular release of ACh have been proposed. Recently, Wessler and coworkers showed that the release of ACh from human placental villi was inhibited by inhibitors of polyspecific organic cation transporters (OCTs) and suggested that OCTs may be involved in the release of ACh from the placenta and other non-neuronal tissues (10).

To test this hypothesis we investigated whether the three subtypes OCT1–3 (also known as *SLC22A1–3*) are capable of transporting ACh, and more specifically, whether they are able to mediate efflux of ACh from cells. Focusing on airway epithelia, we investigated whether the membrane localization of ACh-transporting OCTs is consistent with their proposed role for ACh release. The obtained data suggest that the luminal release of ACh from ciliated epithelial cells in human airways is mainly mediated by OCT2, and that glucocorticoids inhaled during the treatment of asthma can inhibit this function.

MATERIALS AND METHODS

Expression of OCTs in Oocytes of *X. laevis*

For injection into *Xenopus* oocytes, m7G(5′)ppp(5′)G-capped cRNAs were prepared from the cDNAs of OCT1–3 from rat (rOCT1 [11], rOCT2 [12], rOCT3 [13]) and human (hOCT1 [14], hOCT2 [14], hOCT3, also called EMT [15]) using the "mMESSAGE mMACHINE" kit (Ambion, Austin, TX). The restriction enzymes used for linearization of the different cDNA vectors and the RNA polymerases used for transcription were described earlier (12–15). Stage V–VI oocytes were defolliculated with collagenase A and stored for several hours in Ori buffer (5 mM 3-(*N*-morpholino)propanesulfonic acid-NaOH, pH 7.4, 100 mM NaCl, 3 mM KCl, 2 mM $CaCl_2$ and 1 mM $MgCl_2$) containing 50 mg/liter gentamicin. For expression, the oocytes were injected with 50 nl H_2O/oocyte containing 10 ng of the respective cRNA and incubated for 3–5 d at 16°C in Ori buffer containing 50 mg/liter gentamicin.

Transport Measurements in Oocytes with Radioactive Substrates

For tracer uptake measurements, oocytes were incubated at 19°C for 30 min in Ori buffer containing [^{3}H]1-methyl-4-phenylpyridinium (MPP), [^{14}C]tetraethylammonium (TEA), or [^{3}H]acetylcholine (ACh) in the absence or presence of inhibitors. The reaction was stopped with ice-cold Ori buffer containing 100 μM quinine, and oocytes were washed with the same solution. Oocytes were solubilized with 5% (wt/vol) SDS and analyzed for radioactivity. For efflux measurements, oocytes expressing OCTs or noninjected control oocytes were injected at room temperature with 2.5 or 0.25 pmoles of [^{3}H]ACh and directly added to

(*Received in original form November 19, 2004 and in final form March 15, 2005*)

Supported by the Deutsche Forschungsgemeinschaft (Grant Li 1051/1-1 to K.S.L. and Grant SFB 487/A4 to H.K.).

* These authors contributed equally to this work.

Correspondence and requests for reprints should be addressed to Hermann Koepsell, Institute of Anatomy and Cell Biology, Koellikerstr. 6, 97070 Würzburg, Germany. E-mail: Hermann@Koepsell.de

Am J Respir Cell Mol Biol Vol 33. pp 79–88, 2005
Originally Published in Press as DOI: 10.1165/rcmb.2004-0363OC on April 7, 2005
Internet address: www.atsjournals.org

ice-cold Ori buffer. After three times washing with ice-cold Ori buffer, efflux was started by transferring the oocytes to warm Ori buffer (0.2 ml, 19°C). After 1 min incubation, the radioactivity released into the medium and radioactivity remaining in the oocytes were measured.

Electrophysiologic Measurements in Oocytes

Current measurements were performed using the two-electrode voltage-clamp method as described (12, 16). The electrical measurements were started by superfusing the oocytes (room temperature, ~ 2 ml/min) with Ori buffer and clamping their membrane potential to −50 mV. For measurement of currents induced by external ACh, the oocytes were superfused for 30 s with Ori buffer containing the indicated concentrations of ACh, and superfused again with Ori buffer. To measure outwardly directed currents induced by cytoplasmatic ACh, oocytes were clamped to −50 mV and then injected with ACh (2.5 nmoles in 50 nl water). Injection of ACh elicited outward currents that were abolished when the oocytes were superfused with Ori buffer containing 5 mM ACh. With ACh-injected oocytes, similar outward currents were observed when superfusate was switched from 5 mM ACh in Ori to Ori without ACh. The inhibition of ACh induced outward currents by various concentrations of nicotine, corticosterone, beclomethasone, budesonide, or fluticasone was measured with ACh-injected oocytes that were alternately superfused with Ori buffer containing 5 mM ACh and Ori buffer containing increasing concentrations of inhibitors.

Expression of OCTs in Mammalian Epithelial Cells

Generation of a human embryonic kidney (HEK) 293 cell line expressing hOCT2 has been reported (17). HEK 293 cells expressing rOCT1, rOCT2, rOCT3, and hOCT1 were generated in the same way. Cloning of rOCT1, rOCT2, and hOCT1 has been described (11, 12, 14) and rOCT3 and hOCT3 were kindly provided by Dr. V. Ganapathy (13, 18). The transporters were subcloned into pcDNA3.1(+) (Invitrogen GmbH, Karlsruhe, Germany) using either *Kpn*I/*Xba*I or *Hind*III/*Eco*RI restriction sites. hOCT1, hOCT2, and hOCT3 were stably expressed in the Chinese hamster ovary (CHO) cell line CHO-K1 obtained from the American Tissue Culture Collection (ATCC, Manassas, VA). The plasmids were transfected into CHO-K1 cells by incubation with 12 μl Fugene 6 transfection reagent (Roche, Mannheim, Germany) and 4 μg of DNA in 400 μl Optimem buffer (Invitrogen GmbH). Stable transfectants were selected with geneticin G418 (Roche) (17) followed by subcloning. HEK 293 cells were grown in Dulbecco's modified Eagle's medium (F0415; Biochrom, Berlin, Germany) supplemented with 44 mM $NaHCO_3$, 5.5 mM D-glucose and 2 mM L-glutamine. CHO-K1 cells were grown in Iscove medium (F0465; Biochrom) supplemented with 36 mM $NaHCO_3$ and 2 mM glutamine. Both media were gassed with 8% CO_2 and contained 100,000 U/liter penicillin, 100 mg/liter streptomycin, and 0.8 mg/ml G418. Cells were grown to confluence and washed with phosphate-buffered saline (PBS). To prepare the cells for cryosectioning, cells were suspended in PBS, added to a 1.5-ml Eppendorf vial, and centrifuged for 3 min at 8,000 × *g*. The supernatant was removed and the vial was frozen in liquid nitrogen. The frozen pellet was glued to the sample holder of the cryostat and 10-μm-thick cryosections were made.

For transport measurements, confluent cells were washed with PBS, suspended by shaking, collected by 10 min centrifugation at 1,000 × *g*, and suspended at 37°C in PBS. The cells were incubated for 1 s in PBS containing 5 μM [^{3}H]ACh or 0.2 μM [^{3}H]1-methyl-4-phenylpyridinium ([^{3}H]MPP) without inhibitor or with 100 μM quinine. Uptake was stopped by addition of ice-cold PBS containing 100 μM quinine (stop solution), and the cells were washed three times with ice-cold stop solution. To measure uptake at 0 s incubation, ice-cold stop solution was added to the cells first, and radioactive substrates were added thereafter. Uptake rates were calculated from quadruplicate measurements after 0 s incubation and 1 s incubation. They were measured in the absence of quinine or after 10 min preincubation with (and presence of) 100 μM quinine. Quinine inhibited uptake rates were calculated.

Antibodies

For the immunolocalization of rat OCTs, we used previously described affinity-purified antibodies against peptides of rOCT1 and of rOCT2 (19) and affinitiy-purified antibodies against rOCT1, rOCT2, and rOCT3 from Alpha Diagnostic (San Antonio, TX). The antibodies from Alpha Diagnostic were raised against a 21–amino acid sequence near the C-terminus of rOCT1 which has 66% amino acid identity to hOCT1 (anti–rOCT1-Ab), against a 21–amino acid sequence in the large intracellular loop of rOCT2 (anti–rOCT2-Ab), and an 18–amino acid sequence in the large intracellular loop of rOCT3 (anti–rOCT3-Ab). In rat airways, identical results were obtained with the antibodies against rOCT1 and rOCT2 from Alpha Diagnostic as with our own previously described antibodies against rOCT1 and rOCT2 (19). For the immunolocalization of human OCT1, we used the antibody against rOCT1 from Alpha Diagnostic (anti–rOCT1-Ab), which cross-reacts with the human ortholog. For immunolocalization of hOCT2 and hOCT3, antibodies against subtype-specific peptides were raised in rabbits and affinity-purified on the respective antigenic peptides. The antibody against hOCT2 (anti–hOCT2-Ab) was raised against amino acids 533–547 (CQRPRKNKEKMIYLQV) of hOCT2 (14) (Eurogentec, Seraing, Belgium). This sequence is not present in the recently described splice variant hOCT2-A (20). The antibody against hOCT3 also called EMT (anti–hOCT3-Ab) was raised against amino acids 297–313 (TRKKGDKALQILRRIAK) of hOCT3 (15). In Western blots on crude plasma membranes of human kidney and human placenta, anti–hOCT2-Ab and anti–hOCT3-Ab reacted specifically with ~ 80-kD polypeptides. Goat antibody against the vesicular ACh transporter (anti–VAChT-Ab) was obtained from Biotrend (Köln, Germany), and the monoclonal (mouse) antibody against villin (anti–villin-Ab, clone ID2C3) from Immunotech (Marseille, France). As secondary antibodies, Cy3-coupled donkey anti-rabbit Ig from Chemicon (Hofheim, Germany), fluorescein-isothiocyanate (FITC)-conjugated donkey anti-rabbit Ig from Dianova (Hamburg, Germany), FITC-conjugated donkey anti-mouse IgG from Dianova, and FITC-conjugated mouse anti-goat-IgG from Sigma (Deisenhofen, Germany) were used.

Immunofluorescence

Ten-micrometer-thick cryosections were prepared from pellets of HEK 293 or CHO-K1 cells, from rat trachea and lung (n = 5), or from unaffected segments of human bronchi that had been surgically removed due to lung cancer (n = 5). The pellets were frozen in liquid nitrogen and the tissues in melting 2-methylbutane. Cryosections were fixed with acetone at −20°C and incubated for 1 h at room temperature in PBS containing 50% normal porcine serum (pH 7.4). Sections were incubated for 12–16 h at room temperature with affinity-purified primary antibodies diluted in PBS (anti–rOCT1-Ab, 1:20; anti–rOCT2-Ab, 1:400; anti–rOCT3-Ab, 1:200; anti–hOCT2-Ab, 1:100; anti–hOCT3-Ab, 1:500; anti–VAChT-Ab, 1:800; and anti–villin-Ab, 1:100). After washing in PBS, the sections were incubated for 1 h at room temperature with PBS-diluted secondary antibodies (Cy3-coupled donkey anti-rabbit-Ig, 1:2,000; FITC-coupled donkey anti-rabbit-Ig, 1:100; FITC-conjugated mouse anti–goat-IgG, 1: 800; and FITC-conjugated donkey anti-mouse IgG, 1:200). Sections were rinsed with PBS, coverslipped with carbonate-buffered glycerol (pH 8.6) and evaluated by epifluorescence microscopy or with a confocal laser scanning microscope (TCSSP2; Leica, Mannheim, Germany). Negative controls were done by (*1*) omission of first antibody, (*2*) pre-absorption of the primary antibodies with 10–200 μg/ml of their respective antigenic peptides, and (*3*) immunoreaction with cells lines expressing OCT subtypes as described in RESULTS.

RT-PCR

Total RNA was isolated from kidneys and abraded tracheal epithelium of adult Wistar rats (n = 5; Harlan Winkelmann, Borchem, Germany) as well as from human tracheal and bronchial epithelium using the RNeasy kit (Qiagen, Hilden, Germany). The human epithelia were obtained at autopsy from subjects that showed no evidence of lung disease. DNA was digested by DNase I, and 5 μg RNA was reversely transcribed in 20 μl reaction mix by 50 min incubation at 42°C with Superscript RNaseH$^-$ reverse transcriptase (Invitrogen GmbH). The reverse transcriptase was inactivated by heating to 75°C for 15 min. The cDNAs were amplified with the gene-specific primer pairs covering at least one intron (Table 1). For amplification, 2.5 μl buffer II (100 mM Tris-HCl, 500 mM KCl, pH 8.3), 2 μl 15 mM $MgCl_2$, 0.6 μl dNTP (10 mM each), 0.6 μl of each primer (10 μM), and 0.125 μl AmpliTaq Gold polymerase (5 U/μl) were added to 1 μl of reversely transcribed cDNA, and made up to a final volume of 25 μl with H_2O. Cycling conditions were 12 min at 95°C, 40 cycles with 45 s at 95°C,

TABLE 1. OLIGONUCLEOTIDE PRIMERS FOR AMPLIFICATION OF OCTS, VAChT, AND GAPDH

Gene	Accession No.	Primer	Product Length (*bp*)
rOCT1	X78855	Forward: CATCTGTGTCCGGTGTGC	398
		Reverse: CTTCAGGTCAGCAGGAGG	(597–994)
rOCT2	X98334	Forward: GCCTCCTGATCCTGGCTG	226
		Reverse: GGTGTCAGGTTCTGAAGAGAG	(780–1,005)
rOCT3	NM_019230	Forward: TTCGGCGTTGGCATCACG	421
		Reverse: CTGTAACTGTGATCTCTGAG	(944–1,364)
hOCT1	NM_003057	Forward: GACGCCGAGAACCTTGGG	198
		Reverse: GGGTAGGCAAGTATGAGG	(1,648–1,845)
hOCT2	NM_153191	Forward: CTACAGTCCTCATAAATGCTGCAGC	414
		Reverse: GCTGAAGGGAGGCGGGTAGAG	(689–1,102)
hOCT3	NM_021977	Forward: GGAGTTTCGCTCTGTTCAGG	216
		Reverse: GGAATGTGGACTGCCAAGTT	(1,432–1,647)
VAChT	NM_031663	Forward: CCGGTAGGGCATGGAACC	1609
		Reverse: GGTCTGCTAGCTGCGGGAGTA	(848–2,457)
GAPDH	AF199235	Forward: CGTCTTCACCACCATGGAGA	299
		Reverse: CGGCCATCACGCCACAGCTT	(1,143–1,442)

Definition of abbreviations: bp, base pairs; GAPDH, glyceraldehyde-3-phosphate dehydrogenase; hOCT, human organic cation transporters; rOCT, rat organic cation transporters; VAChT, vesicular acetylcholine transporter.

45 s at 55–60°C, 45 s at 72°C, and a final extension at 72°C for 7 min. The PCR products were separated by electrophoresis on a 1.2% agarose gel in TRIS-acetate-EDTA buffer. Sequencing of PCR products was done by MWG Biotech (Ebersbach, Germany). Negative controls were performed by (*1*) omitting the DNA template or (*2*) omitting the reverse transcription step.

Calculations and Statistics

For tracer uptake and efflux measurements, representative experiments are presented in Figures 1A, 1B, and 7A that were performed with three different batches of oocytes. Mean values ± SD of 8–10 individual oocytes (uptake) or of 4 individual oocytes (efflux) are presented. For determination of half-maximal concentrations of ACh-induced currents (Figure 2B) and for determination of IC_{50} values for inhibition of ACh-induced currents (Figures 6B, 7B, 7C) 6–8 oocytes from three different oocyte batches were measured and mean values ± SD of all measured oocytes are presented. Apparent IC_{50} values were obtained from fits of the Hill equation to substrate uptake or substrate-induced currents at different inhibitor concentrations. At the employed experimental conditions (*cis*-inhibition using substrate concentrations more than 10 times smaller compared with the K_M value, or *trans*-inhibition of substrate-induced outward currents), the IC_{50} values are practically identical to the K_i values. The half-maximal values for activation of inward currents by ACh, which represent the K_M values of electrogenic transport, were calculated by fitting the Michaelis Menten equation to the data (Figure 2B). One-way ANOVA followed by Tukey comparison was used to evaluate differences between various groups. The unpaired Student's *t* test was used to test differences of two mean values for statistical significance (GraphPad 4.0, GraphPad Software Inc., San Diego, CA).

Materials

[^{3}H]MPP (3.1 TBq/mmol), [^{14}C]TEA (1.9 GBq/mmol), and [^{3}H]ACh (0.74 TBq/mmol) were obtained from Biotrend (Köln, Germany). Nicotine, budesonide, and beclomethasone diproprionate were purchased from Sigma. Fluticasone was kindly provided by GlaxoSmithKline (München, Germany). All other chemicals were obtained as described earlier (6, 12, 16).

RESULTS

Transport of ACh by OCT1 and OCT2 from Rat and Human

The three OCT subtypes from rat and human were expressed in *Xenopus* oocytes. Uptake of 0.2 μM [^{3}H]MPP and 5 μM [^{3}H]ACh was measured in oocytes expressing OCTs versus noninjected oocytes (Figure 1A). Similar uptake rates of 0.2 μM MPP were expressed by OCT1–3 from rat and human. Significant uptake of 5 μM ACh was also observed with OCT1 and OCT2 from rat and human, but not with OCT3 from rat or human (Figure 1A). In three independent experiments with OCT3 from rat and human, the uptake rates of 5 μM ACh (in pmol × oocyte^{-1} × 30 min^{-1}) were 1.4 ± 0.4 (rOCT3), 1.1 ± 0.3 (hOCT3),

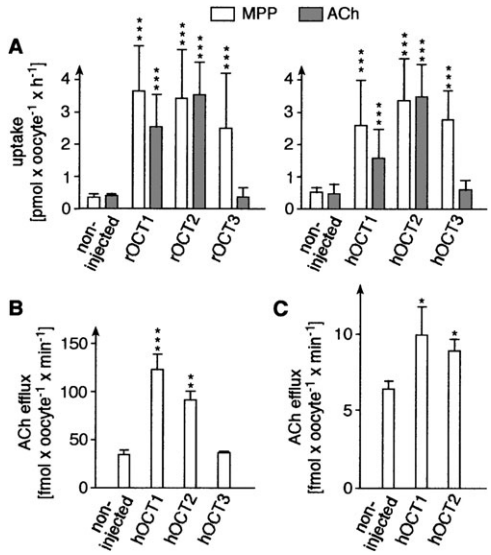

Figure 1. Uptake and efflux of ACh by OCTs expressed in *X. oocytes*. (*A*) Comparison of uptake of 0.2 μM [^{3}H]MPP and 5 μM [^{3}H]ACh by OCT1–3 from rat and human. Uptake was measured over 30 min. Mean values ± SD from 8–10 oocytes are shown. A typical experiment out of three is shown. (*B*) Efflux of ACh from noninjected control oocytes and from oocytes expressing human OCT1–3. Oocytes were injected with 2.5 pmol × oocyte^{-1} [^{3}H]ACh, and the ACh efflux during 1 min incubation into 0.2 ml of Ori buffer was measured. Mean values ± SD from four oocytes are indicated. A typical experiment out of three is shown. (*C*) Efflux of ACh from noninjected oocytes and from oocytes expressing human OCT1 and OCT2. Oocytes were injected with 0.25 pmol × oocyte^{-1} [^{3}H]ACh. ACh efflux was measured and the data are presented as in *B*. Significant differences between uptake rates measured in oocytes expressing OCTs and noninjected oocytes are indicated (ANOVA, *$P < 0.05$, **$P < 0.01$, ***$P < 0.001$).

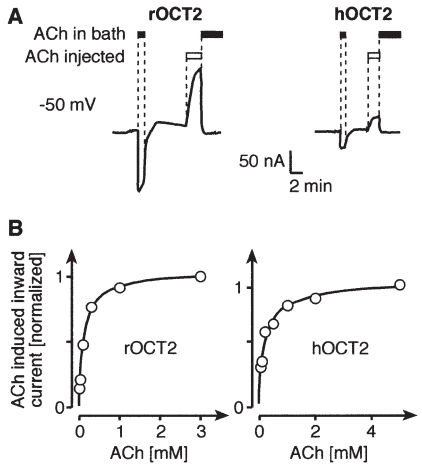

Figure 2. ACh-induced currents mediated by OCT2 from rat and human. rOCT2 or hOCT2 were expressed in *X. oocytes*. (*A*) The oocytes were superfused with Ori buffer and clamped to −50 mV. Inward currents were induced by superfusion with Ori buffer containing 5 mM ACh. Outward currents were induced by injection of 2.5 nmol of ACh per oocyte. Outward currents were blocked by superfusion with 5 mM ACh. (*B*) Inward currents in oocytes expressing rOCT2 or hOCT2 that were induced by superfusion with the indicated concentrations of ACh. The inward currents measured in the individual oocytes were normalized to currents observed with the highest employed concentration of ACh. Mean current ± SD from 6–8 oocytes taken from three separate batches of oocytes are indicated. The Hill equation was fitted to the data.

and 1.1 ± 0.5 (noninjected control oocytes). We also determined the uptake of 0.2 μM [^{3}H]MPP or 5 μM [^{3}H]ACh in CHO cells expressing hOCT1, hOCT2, or hOCT3 and in CHO control cells stably transfected with the empty expression vector pcDNA 3.1 in the absence and presence of 100 μM of the OCT inhibitor quinine (21). Expression of hOCT1 or hOCT2 significantly increased quinine-inhibited uptake of MPP as well as quinine-inhibited uptake of ACh. In contrast, expression of hOCT3 in CHO cells increased quinine inhibited uptake of MPP but not quinine-inhibited uptake of ACh. The following quinine-inhibited uptake rates were measured (means ± SD, $n = 4$, in pmol × mg protein^{-1} × s^{-1}): hOCT1 MPP 1.8 ± 0.1, ACh 1.1 ± 0.2; hOCT2 MPP 3.8 ± 0.1, ACh 6.5 ± 0.5; hOCT3 MPP 5.2 ± 0.4; ACh −0.06 ± 0.14.

To test whether the human OCT transporters are capable of mediating cellular release of ACh, we injected 2.5 pmol [^{3}H]ACh × oocyte^{-1} into oocytes expressing human OCTs or into control oocytes, and measured the efflux of [^{3}H]ACh into the medium during 1 min incubation in Ori buffer (Figure 1B). Assuming that injected [^{3}H]ACh distributes within an internal ocyte volume of 0.5 μl, the initial internal concentration of [^{3}H]ACh was ∼ 5 μM. The efflux was started by transferring the injected oocytes from ice-cold to warm Ori buffer. In three independent experiments, during 1 min incubation significantly more [^{3}H]ACh was released from oocytes expressing hOCT1 and hOCT2 than from noninjected control oocytes, whereas the efflux of injected ACh was not increased by expression of hOCT3. In the noninjected oocytes of Figure 1B, 1.4 ± 0.2% of injected [^{3}H]ACh was released within 1 min. In the oocytes expressing hOCT1 or hOCT2, 3.6 ± 0.7% and 2.3 ± 0.4% of injected [^{3}H]ACh were released in addition (means ± SD). In Figure 1C, we demonstrate hOCT1 and hOCT2 induced [^{3}H]ACh release after injection of 0.25 pmol per oocyte. In this experiment the initial intracellular concentration of [^{3}H]ACh was ∼ 0.5 μM. This concentration ranges between the ACh concentrations measured in ciliated epithelia cells of rat and human airways (22). Also under these conditions significantly higher ACh efflux was observed in oocytes expressing hOCT1 or hOCT2 compared with noninjected oocytes. Taken together, the data in Figure 1 show that hOCT1 as well as hOCT2 can translocate ACh in either direction. In contrast, hOCT3 does not exhibit ACh transport in either direction that could be detected in our assay systems.

To determine the affinity of ACh to the OCTs, we measured uptake of 0.2 μM [^{3}H]MPP by oocytes expressing rOCT1, rOCT2, hOCT1, or hOCT2 in the presence of ACh. The measurements were performed in the presence of eight different concentrations of ACh using 8–10 oocytes per data point. Fitting the Hill equation to the data points, IC_{50} values of 82 ± 17 μM (rOCT1), 153 ± 35 μM (rOCT2), 580 ± 110 μM (hOCT1), and 149 ± 22 μM (hOCT2) were obtained. Note, that the IC_{50} value for hOCT2 was 4-fold lower compared with hOCT1 ($P < 0.001$ for difference). Because the MPP concentration used in these measurements was at least 20 times lower than the K_M values of the OCTs (21), the determined IC_{50} values are about identical to the respective K_i values.

Induction of Membrane Currents in Oocytes Expressing OCT2 by Intracellular versus Extracellular ACh

We expressed OCT2 from rat and human in *Xenopus* oocytes, clamped the oocytes to −50 mV, and investigated the currents induced by superfusion with 5 mM ACh and by injection of 2.5 nmol of ACh. Assuming an even intracellular distribution of injected ACh in an accessible volume of 0.5 μl, this amount of injected ACh would increase the intracellular ACh concentration to ∼ 5 mM. In oocytes expressing rOCT2 or hOCT2, extracellular ACh induced inward currents, and intracellular ACh induced outward currents (Figure 2A). Current amplitudes measured at a clamped membrane potential of −50 mV were comparable for inward versus outward currents. In noninjected control oocytes, neither intracellular nor extracellular ACh induced any currents (data not shown). ACh-induced inward and outward currents were dependent on the membrane potential, as has been previously described for other substrates (16, 17, 21). For example, when an outwardly directed gradient of ∼ 5 mM versus 0 mM ACh was applied to one hOCT2 expressing oocyte, currents of 43 nA, 56 nA, and 90 nA were induced at −100 mV, −50 mV, and 0 mV, respectively. As described previously for other substrates, the currents observed with rOCT2 were higher as compared with hOCT2 (12, 17). For currents induced by extracellular ACh in oocytes expressing rat or human OCT2 at −50 mV, half-maximal activations were observed at ACh concentrations of 175 ± 43 μM (rOCT2) and 117 ± 13 μM (hOCT2) (Figure 2B). These values were not significantly different from the respective IC_{50} values obtained for inhibition of MPP uptake by ACh (*see above*).

Expression and Localization of OCTs in Tracheal and Bronchial Epithelium of Rat and Human

The functional studies showed that cellular release of ACh can be mediated via OCT1 and OCT2. To explore the basis of a putative participation of OCTs in non-neuronal cholinergic signaling by airway epithelial cells (9), we investigated the expression and membrane localization of OCTs in epithelial cells of the trachea and bronchi of rat and human. We performed RT-PCR on bronchial epithelial cells with subtype-specific primers and immunofluorescence labeling of trachea and bronchi using subtype specific antibodies. The antibodies were tested for subtype specific immunohistochemical staining in Figure 3, using

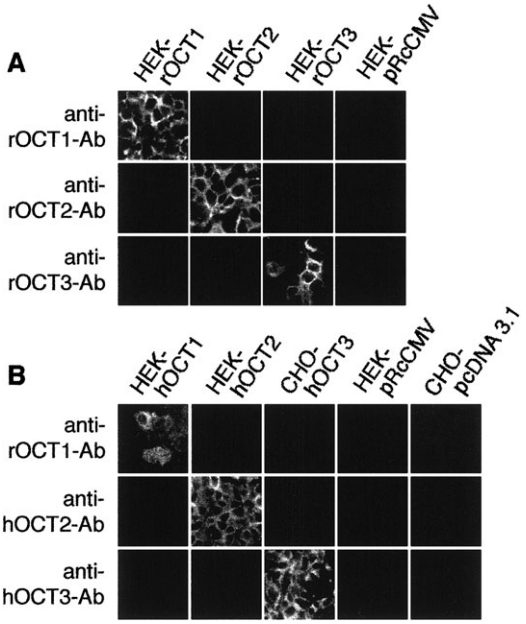

Figure 3. Subtype specificitiy of antibodies for immunostaining of OCT1, OCT2, and OCT3. HEK 293 cells and CHO cells that were stably transfected with expression vectors (HEK-pRcCMV, CHO-pcDNA3.1) or with expression vectors containing individual OCT-subtypes from rat (HEK-rOCT1, HEK-rOCT2, HEK-rOCT3) and human (HEK-hOCT1, HEK-hOCT2, CHO-hOCT3) were grown to 80% confluence, washed, and spun down. The pellets were frozen, cryosectioned, fixed, and immunostained exactly as in subsequent studies of the airway tissue from rat and human. (*A*) Immunofluorescence of cells expressing OCT1–3 from rat using affinity purified antibodies against peptides of rat OCTs (anti–rOCT1-Ab, anti–rOCT2-Ab, anti–rOCT3-Ab). (*B*) Immunofluorescence of cells expressing OCT1–3 from human using one affinity-purified antibody raised against a peptide of rOCT1 that cross-reacts with hOCT1 (anti–rOCT1-Ab) and two affinity-purified antibodies raised against peptides of hOCT2 (anti–hOCT2-Ab) and hOCT3 (anti–hOCT3-Ab).

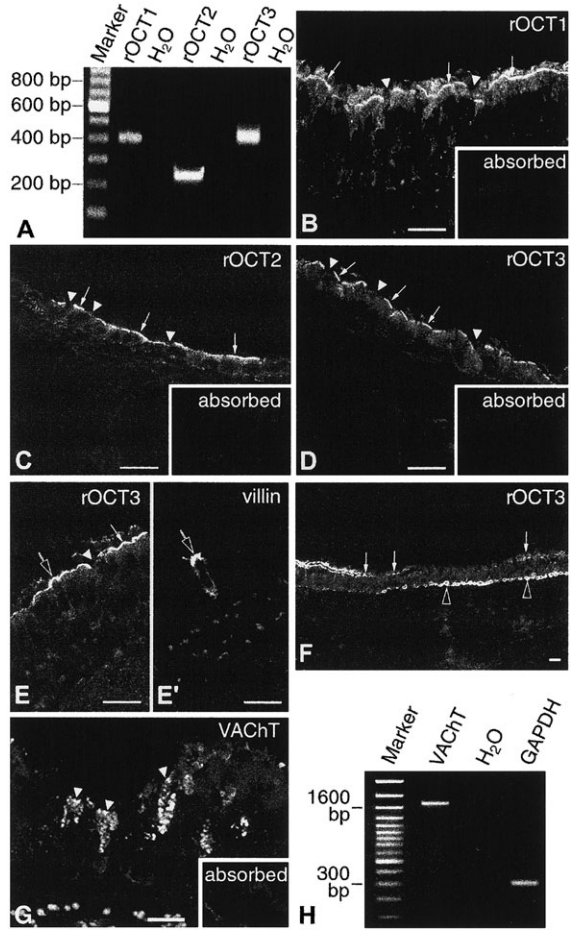

Figure 4. Expression and localization of OCT1–3 and VAChT in rat airway epithelium. (*A*) RT-PCR on abraded tracheal epithelial cells for rOCT1, rOCT2, and rOCT3. The identity of the amplified transporter fragments was verified by sequencing. H_2O, lanes without templates. (*B*) Immunofluorescence detection of anti–rOCT1-Ab in epithelium of rat trachea. The apical membrane of ciliated cells was stained (*arrows*) whereas secretory cells did not show immunoreactivity (*closed arrowheads*). (*C, D*) Immunofluorescence of bronchial epithelium with anti–rOCT2-Ab and anti–rOCT3-Ab. Immunoreactivity for rOCT2 and rOCT3 was concentrated at the apical membrane of ciliated cells whereas secretory cells (*closed arrowheads*) were not stained. (*E, E'*) Double-labeling immunofluorescence with anti-rOCT3-Ab (*E*) and anti-villin-antibody (*E'*), a marker of brush cells. Immunolabeling of rOCT3 in the apical membrane of brush cells was observed (*open arrows*). (*F*) rOCT3-immunostaining of the epithelium at the bifurcation of the trachea. The luminal staining of the ciliated cells (*arrows*) in the stem bronchus (*left hand part of epithelium*) was stronger than in the tracheal carina (*right hand part of epithelium*). The epithelium of the carina contains numerous basal cells that were also labeled with anti–rOCT3-Ab (*open arrowheads*). *Insets* in *B–D* show absorption controls with the corresponding antigenic peptides. *Images* depicted in *B–E* were taken by confocal laser scanning microscopy (CLSM). (*G*) Immunofluorescence detection of VAChT in the tracheal epithelium using anti-VAChT antibody from goat and CLSM. Granules of secretory cells are stained (*closed arrowheads*). (*H*) RT-PCR with abraded tracheal epithelium. With VAChT-specific primers, a fragment of VAChT was amplified and confirmed by DNA sequencing. H_2O, lanes without templates. Amplification of a fragment of glyceraldehyde-3-phosphate (GAPDH). No amplification product was obtained when the reverse transcription of the RNA was omitted whereas an identical amplification product was obtained with rat spinal cord (not shown). *Inset* in *G*: absorption control. *Bars*: 20 μm.

cryosectioned cell pellets from cell lines expressing the different transporters and control cell lines transfected with the expression vectors. For immunostaining of rat tissues, we used antibodies that were raised against peptides of the three OCT subtypes from rat (anti–rOCT1-Ab, anti–rOCT2-Ab, anti–rOCT3-Ab). These antibodies only stained the respective OCT subtype and showed no reaction with HEK-293 cells expressing the empty expression vector (Figure 3A). For immunostaining of OCT1 in human tissue we used anti–rOCT1-Ab. This antibody was raised against a peptide of rOCT1 and cross-reacts with hOCT1 but not with hOCT2 or hOCT3 (Figure 3B). OCT2 and OCT3 in human tissue were stained with antibodies raised against peptides of the human subtypes (anti–hOCT2-Ab, anti–hOCT3-Ab). Similarly, these antibodies showed subtype-specific immunostaining and did not react with vector-transfected control cell lines.

In abradates from rat tracheal epithelium, transcripts coding for rOCT1, rOCT2, and rOCT3 were detected by RT-PCR (Figure 4A). No amplification was observed when the reverse transcription was omitted (not shown). The correspondence of amplified cDNA fragments with the particular OCT subtypes was verified by cDNA sequencing. In epithelia of trachea and bronchi from rat, the apical membrane of ciliated cells was stained by anti–rOCT1-Ab, anti–rOCT2-Ab, and anti–rOCT3-Ab (Figures 4B–4F). In some sections staining of the cilia could be resolved (Figures 4B, 4D, and 4E). Identical results were ob-

tained with trachea versus bronchi. Immunolabeling could be blocked by preincubation with the respective antigenic peptide (*inserts* in Figures 4B–4D). rOCT1 and rOCT2 protein were not detected in other epithelial cell types of the airways, whereas rOCT3 was also present in villin-positive brush cells (Figures 4E and 4E′) and in basal cells (Figure 4F). In rat, basal cells only occur in circumscribed regions of the rat lower airways such as the tracheal carina shown in Figure 4F. In brush cells, rOCT3 is localized only in the luminal membrane, whereas in nonpolarized basal cells rOCT3 is expressed allover the plasma membrane (*arrowheads* in Figure 4F).

To determine whether rat tracheal epithelial cells that express OCTs in the luminal membrane contain cholinergic vesicles that provide another route for luminal release of ACh, we performed immunostaining with an antibody against the vesicular ACh transporter VAChT. VAChT immunoreactivity was observed as expected in cholinergic nerve terminals that innervate primarily the tracheal and bronchial smooth muscle and glands (not shown). In addition, we observed VAChT immunoreactivity in goblet cells of the tracheal epithelium but not in cilated epithelial cells (Figure 4G). The expression of VAChT in (goblet cells of) rat tracheal epithelium was confirmed by RT-PCR on abraded tracheal epithelial cells (Figure 4H).

RT-PCR on abraded epithelial cells from human trachea and human bronchi showed the presence of transcripts of OCT1, OCT2, and OCT3 (Figure 5A). No amplification of products was observed without reverse transcription of the mRNAs (data not shown). By immunofluorescence of human bronchi using anti–rOCT1-Ab that cross-reacts with hOCT1, intracellular staining of ciliated epithelial cells was observed (Figure 5B). In addition, there was labeling for hOCT1 in the luminal membrane of ciliated epithelial cells (*see arrows* in Figure 5B). OCT2 was mainly detected in the apical membrane of ciliated cells (Figure 5C), and, less intensely, at the plasma membrane of basal cells. Staining of human bronchi for OCT3 revealed weak immunoreactivity of the apical membrane of ciliated cells (arrows in Figure 5D). In contrast, the entire plasma membrane of basal cells and the basolateral membrane of intermediate cells were stained more intensely (Figure 5D).

Inhibition of hOCT2 by Corticosterone and Nicotine

The above findings suggested that OCT2 is important for the luminal release of ACh from ciliated cells in human bronchi. This opened the possibility that nicotine or glucocorticosteroids interfere with cholinergic regulations by inhibiting the hOCT2-dependent release of ACh. The inhibition of hOCT2 may impede bronchociliary clearance and the regeneration of bronchial epithelial cells (2, 3, 9). We therefore measured the effect of various concentrations of corticosterone or nicotine on the uptake of 1 μM [^{14}C]TEA. For these measurements, the oocytes were preincubated for 10 min with the inhibitors, followed by uptake of [^{14}C]TEA over 30 min in the presence of the inhibitors (8–10 oocytes were measured for each concentration of inhibitor). Fitting the Hill equation to the data, IC_{50} values of 47 ± 3 μM and 42 ± 3 μM were obtained for corticosterone and nicotine, respectively. For the inhibition of MPP uptake (25 nM) by corticosterone measured in human embryonic kidney cells expressing hOCT2, a similar IC_{50} value of 34 ± 7 has been reported (23).

In oocytes expressing rOCT2, we recently observed a 30-fold lower affinity for the *cis*-inhibition by corticosterone of cation uptake compared with the *trans*-inhibition by corticosterone of cation efflux (16). This difference was explained by assuming an additional conformational state of the empty transporter that exhibits a high affinity for corticosterone. To determine whether the affinities for the inhibition of hOCT2 mediated ACh efflux by corticosterone and nicotine are higher than the affinities observed for the inhibition of uptake, we measured ACh-induced outward currents in *Xenopus* oocytes expressing hOCT2 at −50 mV in the presence of various concentrations of corticosterone (Figure 6) or nicotine (data not shown) in the superfusate. For the inhibition of ACh efflux by corticosterone, an IC_{50} value of 2.1 ± 0.5 μM (mean ± SD, $n = 6$) was obtained. This value is 22 times lower than the value measured for the inhibition of cation uptake by hOCT2 (*see above*). At variance, nicotine inhibited ACh efflux with an IC_{50} value of 40 ± 5 μM (mean ± SD, $n = 6$). This value is not significantly different from the IC_{50} value of 42 μM determined for inhibition of TEA uptake (*see above*). Whereas the nicotine concentrations in bronchial epithelia achieved by smoking are probably not high enough to inhibit hOCT2 (24), the relatively high affinity of corticosterone for the inhibition of ACh efflux by hOCT2 pointed to the possibility that therapeutic doses of inhaled glucocorticoids can inhibit hOCT2-mediated ACh release.

Inhibition of hOCT1 and hOCT2 by Inhalational Glucocorticoids

We investigated whether uptake of 1 μM [^{14}C]TEA expressed by hOCT1 or hOCT2 were inhibited by 10 μM or 100 μM of the inhalational glucocorticoids beclomethasone, budesonide, or fluticasone (Figure 7A). No significant inhibition of hOCT1

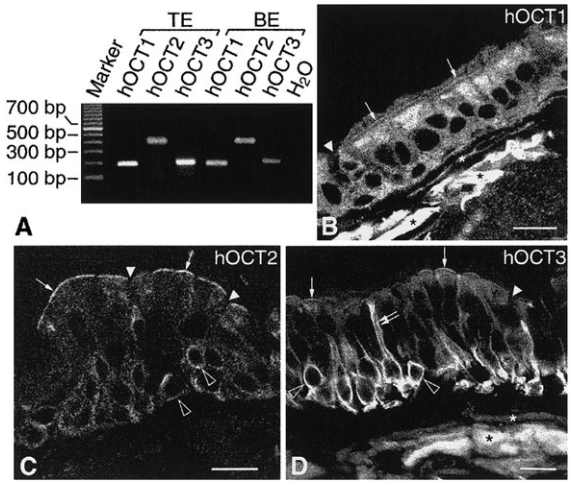

Figure 5. Expression and localization of OCT1–3 in human airway epithelium. (*A*) RT-PCR was performed with abraded tracheal (TE) and bronchial epithelium (BE) using primers that are specific for human OCT subtypes. The amplified OCT-fragments were confirmed by sequencing. (*B–D*) Immunostaining of bronchial epithelium using anti–rOCT1-Ab (hOCT1), anti–hOCT2-Ab (hOCT2), and anti–hOCT3-Ab (hOCT3) and CLSM. Elastic fibers in *B* and *D* (*asterisks*) exhibit autofluorescence. Cellular fluorescence shown in *B–D* was blocked completely when the antibodies were pre-absorbed with their respective antigenic peptides. Immunoreactivity of hOCT1 (*B*) was mainly observed within the epithelial cells; however, weak staining of the apical membrane of ciliated cells (*arrows*) was also detected. Goblet cells (*closed arrowhead*) were not stained. Immunoreactivity of hOCT2 (*C*) was mainly located in apical membrane of ciliated cells (*arrows*), whereas goblet cells were not stained (*closed arrowheads*). Weak staining for hOCT2 was also observed in the basal cells (*open arrowheads*). Immunoreactivity of hOCT3 (*D*) was located in plasma membranes of basal cells (*open arrowheads*), in the basolateral membrane of intermediate cells (*double arrow*), and in the apical membrane of ciliated cells (*arrows*). After preabsorption of the antibodies with their antigenic peptides, no immunostaining of hOCT1, hOCT2, and hOCT3 in the bronchial epithelial cells was observed (not shown). *Bars*: 20 μm.

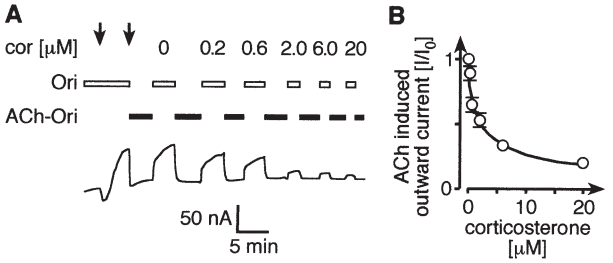

Figure 6. Inhibition of hOCT2-mediated ACh efflux by corticosterone. hOCT2 was expressed in *X.* oocytes. (*A*) Current trace from one oocyte in which the outward current induced by cytoplasmic ACh was inhibited by various concentrations of extracellular corticosterone (*trans*-inhibition). The oocyte was superfused with Ori buffer (Ori), clamped to −50 mV, and injected with 2.5 nmol ACh (the *two arrows* indicate the injection period). ACh injection led to an outward current that was blocked when the superfusate was switched to Ori buffer containing 5 mM ACh (ACh-Ori) and re-appeared when the oocyte was superfused with Ori buffer. *Trans*-inhibition of ACh induced outward currents was measured by adding increasing concentrations of corticosterone (cor) during superfusion periods with Ori buffer. (*B*) Concentration dependence of *trans*-inhibition of ACh-induced outward currents by corticosterone. Mean values ± SD of six oocytes from three oocyte batches are indicated. The Hill equation was fitted to the data.

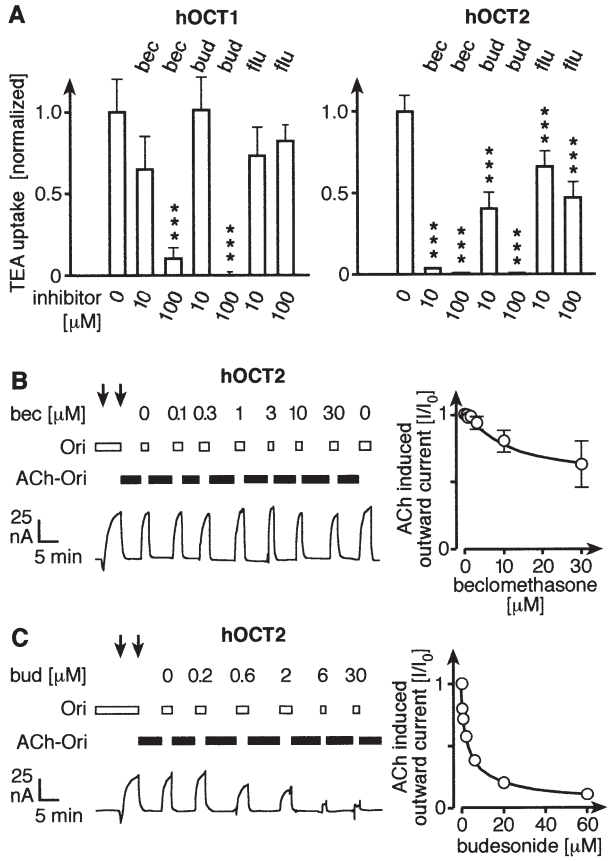

Figure 7. Effects of inhalational glucocorticoids on TEA uptake by hOCT1 or hOCT2 and on ACh efflux by hOCT2. (*A*) In oocytes expressing hOCT1 or hOCT2, and in noninjected oocytes, uptake of 1 μM [^{14}C]TEA was measured over 30 min. Measurements were performed in the absence and presence of the indicated inhibitors beclomethasone (bec), budesonide (bud), and fluticasone (flu). Expressed uptake rates were calculated by subtracting the uptake rates measured in noninjected oocytes. A typical experiment out of three performed with different oocyte batches is shown. Mean uptake values from 7–10 oocytes ± SD are presented. Significant differences between uptake rates measured in the absence and presence of inhibitor are indicated (ANOVA, ***$P <$ 0.001). (*B*) *Trans*-inhibition of hOCT2-expressed ACh-mediated outward current by various concentrations of beclomethasone. The experiment was performed and is presented as in Figure 6. The typical current trace shown in the *left panel* indicates that similar ACh-induced outward currents were measured at beginning and end of the experiment. In the *right panel,* mean values ± SD from seven oocytes taken from three oocyte batches are shown. (*C*) *Trans*-inhibition of hOCT2 mediated ACh efflux by budesonide. The experiment was performed and is presented as in Figure 6. The *right panel* shows mean values ± SD from six oocytes of three separate batches.

was obtained by 10 μM beclomethasone, 10 μM budesonide, or 100 μM fluticasone; however, TEA uptake was inhibited to 90% by 100 μM beclomethasone and almost completely by 100 μM budesonide. TEA uptake expressed by hOCT2 was more sensitive. A 96% inhibition of hOCT2 was observed with 10 μM beclomethasone, whereas 60% inhibition was obtained with 10 μM budesonide. Fluticasone interacts also with hOCT2 but has a lower affinity compared with beclomethasone and budesonide. With 100 μM fluticasone, TEA uptake by hOCT2 was inhibited ∼ 50%. Measuring the inhibition of hOCT2-mediated TEA (1 μM) uptake by various concentrations of beclomethasone or budesonide, we determined an IC_{50} of 4.4 ± 0.4 μM for beclomethasone and an IC_{50} of 7.3 ± 0.6 μM for budesonide.

Since some compounds including corticosterone inhibit cation transport by OCT2 with different affinities for uptake versus efflux (*see above*) it was important to determine the affinity of the inhalational glucocorticoids for inhibition of ACh efflux by hOCT2. In Figures 7B and 7C, we measured *trans*-inhibition of ACh induced outward currents by various concentrations of beclomethasone and budesonide. In these experiments an outwardly directed gradient of ∼5 mM ACh versus 0 mM ACh was applied and the oocytes were clamped to −50 mV. Only ∼ 40% *trans*-inhibition was obtained with 30 μM beclomethasone (Figure 7B), whereas ACh-induced outward currents by hOCT2 were ∼ 90% *trans*-inhibited with 20 μM budesonide (Figure 7C). For *trans*-inhibition with budesonide, an IC_{50} of 2.7 ± 0.4 μM (mean ± SD, $n = 7$, oocytes from three batches) was determined. In hOCT2-expressing oocytes, we did not observe significant *trans*-inhibition of ACh induced outward currents (outwardly directed ACh gradient of ∼ 5 mM versus 0 mM ACh, −50 mV) when 100 μM fluticasone was added to the superfusate (data not shown). The data indicated that beclomethasone and fluticasone inhibit ACh efflux by hOCT2 with a lower affinity compared with cation uptake. At variance budesonide behaves similar to corticosterone; it inhibits ACh efflux by hOCT2 with a higher affinity compared with cation uptake.

DISCUSSION

This work shows that OCT1 and OCT2 are able to mediate cellular release of ACh, whereas OCT3 does not transport ACh. In the airways, all three OCT subtypes were observed in the luminal membrane of ciliated epithelial cells. Because ciliary epithelial cells are sites of important autocrine and paracrine non-neuronal cholinergic regulations but do not contain storage vesicles for ACh (9) and we could not detect the vesicular acetylcholine transporter (VAChT) in rat ciliary epithelial cells, our data support the hypothesis of Wessler and coworkers, saying that OCT-type transporters are responsible for non-neuronal

ACh release (10). These authors observed that the release of ACh from isolated villi of human placenta was inhibited by inhibitors of OCTs. They suggested that OCT1 and OCT3 are responsible for ACh release from the placenta. Because our data show that ACh is not a substrate of OCT3, only OCT1 may mediate the release of ACh from placenta. For luminal release of ACh in the airways, both OCT1 and OCT2 are supposed to be important. We also report that efflux of ACh by OCT2 from human is *trans*-inhibited by micromolar concentration of the inhalational glucocorticosteroid budesonide used for the treatment of asthma.

The three OCT transporter subtypes are expressed in epithelia of various tissues and in neurons, and are capable of translocating a variety of endogenous and exogenous compounds in both directions (21). They have a broadly overlapping substrate specificity but exhibit distinct differences in affinity for some compounds. There is convincing evidence that these transporters are critically involved in the hepatic and renal excretion of cationic drugs. In contrast, the role of OCT transporters in handling endogenous compounds is understood only poorly. OCT1 and OCT2 are supposed to mediate the first step in the hepatic and renal excretion of cationic drugs because rOCT1, rOCT2, and hOCT2 were located to the basolateral membrane of renal proximal tubules and rOCT1 was detected in the sinusoidal membrane of hepatocytes, and because targeted disruption of OCT1 and/or OCT2 in mice reduced hepatic and renal excretion of some organic cations (reviewed in Ref. 21).

The presence of rOCT1, hOCT2, mouse OCT3 (mOCT3), and rOCT3 in neurons and the capability of the OCTs to transport monoamine neurotransmitters (reviewed in Ref. 21) suggested that OCTs play a role in the termination and/or modulation of synaptic transmission. The importance of OCT3 for CNS function was recently emphasized (25). Vialou and coworkers showed that mOCT3 is expressed in neurons of the area postrema that is involved in the regulation of salt and water ingestion, and that the salt and water uptake of mice was changed after targeted disruption of *mOct3.* OCT3 is also expressed in smooth muscle, for example in smooth muscle of bronchial arteries, where it is involved in the uptake of norepinephrine that terminates sympathetic vasoconstriction (26).

Recently, Sweet and coworkers proposed that OCT2 participates in the clearance of choline from the cerebrospinal fluid by the choroid plexus (27). These authors observed that a fusion protein between green fluorescent protein (GFP) and rOCT2 was targeted to the luminal membrane of transfected epithelial cells in the choroid plexus, and that choline uptake by the choroid plexus was inhibited by inhibitors of OCTs.

The expression of OCT1 and OCT2 in the luminal membrane of ciliated epithelial cells, of OCT2 in the luminal membrane of the choroid plexus, and of OCT1 and OCT2 in the basolateral membrane of renal proximal tubules indicates tissue-dependent membrane targeting. This increases the possible physiologic roles of OCTs. Targeting to the luminal or basolateral membrane of epithelial cells in different tissues has been also demonstrated for other transporters such as the Na^+-D-glucose cotransporter SGLT1 (28).

The data presented in this work clearly show that OCT1 and OCT2 are capable to mediate cellular efflux of ACh from cells. ACh efflux was demonstrated by electrical measurements using unphysiologic high intracellular ACh concentrations and by tracer flux measurements using intracellular ACh concentrations that were $\sim$ 6-fold lower than the ACh concentration measured in ciliated respiratory epithelia of rat (22). Although we were not able to perform efflux measurements with the very low intracellular ACh concentration measured for human ciliated epithelial cells (22), it is very likely that hOCT1 and hOCT2 mediate ACh release from human ciliated epithelial *in vivo*. Recent studies indicate that the functional properties of OCT2 are not described sufficiently well by a simple facilitated diffusion system for cations that operates in both directions as previously assumed (21). We observed (*1*) that outward currents induced by cation efflux via rOCT2 at -50 mV were larger compared with inward currents induced by cation influx at -50 mV (12), and (*2*) that the stoichiometry between the translocation of cations and electric charge by rOCT2 exhibited significant deviations from unity (B. M. Schmitt, P. Schlachtbauer, and H. Koepsell, unpublished data). Taken together, the mechanism for cation translocation by OCTs in either direction across the plasma membrane is still poorly understood. Site-directed mutagenesis in rOCT1 and modeling of the tertiary structure of rOCT1—using the crystal structure of lactose permease from *Escherichia coli* that belongs to the same superfamily as the OCTs—indicated that the OCTs contain binding regions with individual substrate binding sites that exhibit allosteric interactions, which may lead to drastic increase in affinity of distinct substrates (29). Such allosteric interaction between endogeneous ligands and the ACh binding site may decrease the K_M for the efflux of ACh.

Assuming electrogenic efflux of ACh by OCTs without coupling to efflux of anions or influx of other cations, a drop of at least 10-fold in ACh concentration from inside to outside is required to overcome a membrane potential of -60 mV according to the Nernst equation. This may be easily achieved—locally or temporarily—because extracellular ACh is rapidly degraded by acetylcholine esterase (AChE). In addition, electrogenic efflux of ACh from ciliated epithelial cells is facilitated by depolarization. Depolarization may be induced by choline uptake via the sodium- and chloride-dependent choline transporter CHT1 or via OCT transporters (6, 21). Extracellular choline may also accelerate ACh efflux via OCT1 or OCT2 due to *trans*-stimulation of these transporters (21). It is a challenge for future studies to investigate the OCT-mediated luminal efflux of ACh *in vivo*. It is also important to determine the ultrastructural distribution of OCT2 within the plasma membrane in relation to the ACh receptors, the AChE, and CHT1 because a close association of OCT2 with the receptor and a more distant localization of AChE would support the proposed coordinated functions.

In airway epithelial cells, the non-neuronal cholinergic system operates independently from the neuronal parasympathetic innervation that maintains a certain cholinergic tonus in smooth muscle cells and glands, and represents the efferent pathway of regulatory circuits (2, 9). Airway epithelial cells express the ACh-synthesizing enzyme ChAT, the ACh-inactivating enzyme AChE, nicotinic and muscarinic acetylcholine receptors (30), and the transporter CHT1, a sodium- and chloride-dependent high-affinity re-uptake system for choline (6). The ciliated epithelial cells do not contain ACh-filled vesicles but are able to release ACh (9). In rat, we showed that they also do not contain the vesicular ACh uptake system VAChT. We found that immunoreactivity of VAChT was restricted to goblet cells in rat bronchial epithelium. However, variations in the expression of VAChT in different species or during development cannot be excluded. In a recent paper, Proskocil and coworkers reported immunostaining of VAChT in the bronchial epithelium of newborn monkeys (31). Unfortunately, the presented pictures do not allow the reader to distinguish between the localization of VAChT in ciliated versus goblet cells.

ACh released from epithelial cells has been shown to increase the proliferation rate of primary cultured bronchial epithelial cells and small cell lung carcinoma cells (2, 4), to increase the ciliary beat frequency in dog bronchial mucosa via muscarinic ACh receptors (3, 32), and to suppress net Na^+ absorption in sheep tracheal epithelium (33). In addition, ACh release from

bronchial epithelial cells inhibits the discharge of mast cells (34). On the other hand, the release of ACh from bronchial epithelial cells has been suggested to mediate bronchoconstriction following the release of serotonin from mast cells (35, 36).

To elucidate whether the inhalation of the glucocorticoids during the treatment of asthma can lead to an inhibition of ACh release from bronchial epithelial cells, we investigated the interaction of beclomethasone, budesonide, and fluticasone with hOCT1 and hOCT2. Because previous experiments with OCT2 from rat revealed different affinities for the *cis*-inhibition of cation uptake versus *trans*-inhibition of cation efflux by corticosterone (16), corticosterone and the three inhalational glucocorticoids were tested for inhibition of TEA uptake by hOCT1 and hOCT2 and for *trans*-inhibition of ACh-induced outward currents by hOCT2. *Trans*-inhibition was only investigated for hOCT2 because we routinely obtained five times higher electrical currents with this transporter than with hOCT1, and efflux measurements with radioactively labeled ACh are technically difficult. Importantly, we observed that corticosterone and budesonide inhibit ACh efflux by human OCT2 with a higher affinity compared with cation influx. At variance, micromolar concentrations of beclomethasone inhibited hOCT2-mediated cation influx but had no significant effect on ACh efflux. We found an IC_{50} value of 2.7 μM for the inhibition of ACh-induced outward currents by budesonide. Given this high affinity, it seems likely that inhalation of this compound will inhibit considerably the efflux of ACh from bronchial epithelial cells. Assuming that the typical single dose of budesonide (~0.5–1 μmol) is dissolved within 100 ml of fluid and mucus covering bronchial epithelial cells, ACh efflux by the bronchial epithelial cells should be blocked by 60–80%. Inhibition of hOCT2 in the bronchial epithelium is supposed to reduce the bronchociliary clearance, to disinhibit mast cells, and to inhibit regeneration of the epithelial cells (9).

Conflict of Interest Statement: None of the authors have a financial relationship with a commercial entity that has an interest in the subject of this manuscript.

Acknowledgments: The authors thank T. Papadakis, I. Schatz, and S. Tasch for expert technical assistance and K. Michael and M. Christof for preparing the figures.

References

1. Reinheimer T, Bernedo P, Klapproth H, Oelert H, Zeiske B, Racké K, Wessler I. Acetylcholine in isolated airways of rat, guinea pig, and human: species differences in role of airway mucosa. *Am J Physiol* 1996;270:L722–L728.
2. Wessler I, Kirkpatrick CJ, Racké K. Non-neuronal acetylcholine, a locally acting molecule, widely distributed in biological systems: expression and function in humans. *Pharmacol Ther* 1998;77:59–79.
3. Wong LB, Miller IF, Yeates DB. Stimulation of ciliary beat frequency by autonomic agonists: in vivo. *J Appl Physiol* 1988;65:971–981.
4. Song P, Sekhon HS, Jia Y, Keller JA, Blusztajn JK, Mark GP, Spindel ER. Acetylcholine is synthesized by and acts as an autocrine growth factor for small cell lung carcinoma. *Cancer Res* 2003;63:214–221.
5. Okuda T, Haga T, Kanai Y, Endou H, Ishihara T, Katsura I. Identification and characterization of the high-affinity choline transporter. *Nat Neurosci* 2000;3:120–125.
6. Pfeil U, Lips KS, Eberling L, Grau V, Haberberger RV, Kummer W. Expression of the high-affinity choline transporter, CHT1, in the rat trachea. *Am J Respir Cell Mol Biol* 2003;28:473–477.
7. Fujii T, Yamada S, Watanabe Y, Misawa H, Tajima S, Fujimoto K, Kasahara T, Kawashima K. Induction of choline acetyltransferase mRNA in human mononuclear leukocytes stimulated by phytohemagglutinin, a T-cell activator. *J Neuroimmunol* 1998;82:101–107.
8. Ogawa H, Fujii T, Watanabe Y, Kawashima K. Expression of multiple mRNA species for choline acetyltransferase in human T-lymphocytes. *Life Sci* 2003;72:2127–2130.
9. Wessler IK, Kirkpatrick CJ. The non-neuronal cholinergic system: an emerging drug target in airways. *Pulm Pharmacol Ther* 2001;14:423–434.
10. Wessler I, Roth E, Deutsch C, Brockerhoff P, Bittinger F, Kirkpatrick CJ, Kilbinger H. Release of non-neuronal acetylcholine from the isolated human placenta is mediated by organic cation transporters. *Br J Pharmacol* 2001;134:951–956.
11. Gründemann D, Gorboulev V, Gambaryan S, Veyhl M, Koepsell H. Drug excretion mediated by a new prototype of polyspecific transporter. *Nature* 1994;372:549–552.
12. Arndt P, Volk C, Gorboulev V, Budiman T, Popp C, Ulzheimer-Teuber I, Akhoundova A, Koppatz S, Bamberg E, Nagel G, *et al.* Interaction of cations, anions, and weak base quinine with rat renal cation transporter rOCT2 compared with rOCT1. *Am J Physiol Renal Physiol* 2001; 281:F454–F468.
13. Kekuda R, Prasad PD, Wu X, Wang H, Fei Y-J, Leibach FH, Ganapathy V. Cloning and functional characterization of a potential-sensitive, polyspecific organic cation transporter (OCT3) most abundantly expressed in placenta. *J Biol Chem* 1998;273:15971–15979.
14. Gorboulev V, Ulzheimer JC, Akhoundova A, Ulzheimer-Teuber I, Karbach U, Quester S, Baumann C, Lang F, Busch AE, Koepsell H. Cloning and characterization of two human polyspecific organic cation transporters. *DNA Cell Biol* 1997;16:871–881.
15. Gründemann D, Schechinger B, Rappold GA, Schömig E. Molecular identification of the corticosterone-sensitive extraneuronal catecholamine transporter. *Nat Neurosci* 1998;1:349–351.
16. Volk C, Gorboulev V, Budiman T, Nagel G, Koepsell H. Different affinities of inhibitors to the outwardly and inwardly directed substrate binding site of organic cation transporter 2. *Mol Pharmacol* 2003; 64:1037–1047.
17. Busch AE, Karbach U, Miska D, Gorboulev V, Akhoundova A, Volk C, Arndt P, Ulzheimer JC, Sonders MS, Baumann C, *et al.* Human neurons express the polyspecific cation transporter hOCT2, which translocates monoamine neurotransmitters, amantadine, and memantine. *Mol Pharmacol* 1998;54:342–352.
18. Wu X, Huang W, Ganapathy ME, Wang H, Kekuda R, Conway SJ, Leibach FH, Ganapathy V. Structure, function, and regional distribution of the organic cation transporter OCT3 in the kidney. *Am J Physiol Renal Physiol* 2000;279:F449–F458.
19. Karbach U, Kricke J, Meyer-Wentrup F, Gorboulev V, Volk C, Loffing-Cueni D, Kaissling B, Bachmann S, Koepsell H. Localization of organic cation transporters OCT1 and OCT2 in rat kidney. *Am J Physiol Renal Physiol* 2000;279:F679–F687.
20. Urakami Y, Akazawa M, Saito H, Okuda M, Inui K-I. cDNA cloning, functional characterization, and tissue distribution of an alternatively spliced variant of organic cation transporter hOCT2 predominantly expressed in the human kidney. *J Am Soc Nephrol* 2002;13:1703–1710.
21. Koepsell H, Schmitt BM, Gorboulev V. Organic cation transporters. *Rev Physiol Biochem Pharmacol* 2003;150:36–90.
22. Reinheimer T, Munch M, Bittinger F, Racke K, Kirkpatrick CJ, Wessler I. Glucocorticoids mediate reduction of epithelial acetylcholine content in the airways of rats and humans. *Eur J Pharmacol* 1998;349:277–284.
23. Hayer-Zillgen M, Brüss M, Bönisch H. Expression and pharmacological profile of the human organic cation transporters hOCT1, hOCT2 and hOCT3. *Br J Pharmacol* 2002;136:829–836.
24. Lindell G, Farnebo LO, Chen D, Nexo E, Rask Madsen J, Bukhave K, Graffner H. Acute effects of smoking during modified sham feeding in duodenal ulcer patients: an analysis of nicotine, acid secretion, gastrin, catecholamines, epidermal growth factor, prostaglandin E_2, and bile acids. *Scand J Gastroenterol* 1993;28:487–494.
25. Vialou V, Amphoux A, Zwart R, Giros B, Gautron S. Organic cation transporter 3 (Slc22a3) is implicated in salt-intake regulation. *J Neurosci* 2004;24:2846–2851.
26. Horvath G, Sutto Z, Torbati A, Conner GE, Salathe M, Wanner A. Norepinephrine transport by the extraneuronal monoamine transporter in human bronchial arterial smooth muscle cells. *Am J Physiol Lung Cell Mol Physiol* 2003;285:L829–L837.
27. Sweet DH, Miller DS, Pritchard JB. Ventricular choline transport: a role for organic cation transporter 2 expressed in choroid plexus. *J Biol Chem* 2001;276:41611–41619.
28. Elfeber K, Stümpel F, Gorboulev V, Mattig S, Deussen A, Kaissling B, Koepsell H. Na^+-D-glucose cotransporter in muscle capillaries increases glucose permeability. *Biochem Biophys Res Commun* 2004; 314:301–305.
29. Popp C, Gorboulev V, Müller TD, Gorbunov D, Shatskaya N, Koepsell H. Amino acids critical for substrate affinity of rat organic cation transporter 1 line the substrate binding region in a model derived from the tertiary structure of lactose permease. *Mol Pharmacol* 2005; 67:1600–1611.
30. Maus ADJ, Pereira EFR, Karachunski PI, Horton RM, Navaneetham D, Macklin K, Cortes WS, Albuquerque EX, Conti-Fine BM. Human

and rodent bronchial epithelial cells express functional nicotinic acetylcholine receptors. *Mol Pharmacol* 1998;54:779–788.
31. Proskocil BJ, Sekhon HS, Jia Y, Savchenko V, Blakely RD, Lindstrom J, Spindel ER. Acetylcholine is an autocrine or paracrine hormone synthesized and secreted by airway bronchial epithelial cells. *Endocrinology* 2004;145:2498–2506.
32. Salathe M, Lipson EJ, Ivonnet PI, Bookman RJ. Muscarinic signaling in ciliated tracheal epithelial cells: dual effects on Ca^{2+} and ciliary beating. *Am J Physiol* 1997;272:L301–L310.
33. Acevedo M. Effect of acetyl choline on ion transport in sheep tracheal epithelium. *Pflugers Arch* 1994;427:543–546.
34. Reinheimer T, Baumgärtner D, Höhle K-D, Racké K, Wessler I. Acetylcholine via muscarinic receptors inhibits histamine release from human isolated bronchi. *Am J Respir Crit Care Med* 1997;156:389–395.
35. Struckmann N, Schwering S, Wiegand S, Gschnell A, Yamada M, Kummer W, Wess J, Haberberger RV. Role of muscarinic receptor subtypes in the constriction of peripheral airways: studies on receptor-deficient mice. *Mol Pharmacol* 2003;64:1444–1451.
36. Moffatt JD, Cocks TM, Page CP. Role of the epithelium and acetylcholine in mediating the contraction to 5-hydroxytryptamine in the mouse isolated trachea. *Br J Pharmacol* 2004;141:1159–1166.